Automatic Diagnosis of Tuberculosis Disease Based on Plasmonic ELISA and Color-based Image Classification

Kamal J. AbuHassan, *Member, IEEE* Noremylia M. Bakhori, Norzila Kusnin, Umi Z. M. Azmi, Marzia H. Tania, Benjamin A. Evans, Nor A. Yusof, M. A. Hossain *Member, IEEE*

***Abstract*— Tuberculosis (TB) remains one of the most devastating infectious diseases and its treatment efficiency is majorly influenced by the stage at which infection with the TB bacterium is diagnosed. The available methods for TB diagnosis are either time consuming, costly or not efficient. This study employs a signal generation mechanism for biosensing, known as Plasmonic ELISA, and computational intelligence to facilitate automatic diagnosis of TB. Plasmonic ELISA enables the detection of a few molecules of analyte by the incorporation of smart nanomaterials for better sensitivity of the developed detection system. The computational system uses k-means clustering and thresholding for image segmentation. This paper presents the results of the classification performance of the Plasmonic ELISA imaging data by using various types of classifiers. The five-fold cross-validation results show high accuracy rate (>97%) in classifying TB images using the entire data set. Future work will focus on developing an intelligent mobile-enabled expert system to diagnose TB in real-time. The intelligent system will be clinically validated and tested in collaboration with healthcare providers in Malaysia.**

I. Introduction

In 2016, TB was still among leading causes of death worldwide [1]. TB represents a public health concern in Malaysia and in many neighboring countries, with a current incidence annual rate of 89/100,000 [2]. The available methods for TB diagnosis are either time consuming, costly or not efficient. According to the Malaysian Thoracic Society (MTS), the diagnosis of post-primary pulmonary tuberculosis, which is the most frequent TB among Malaysian adults may take 72 hours to 8 weeks [3]. The Mantoux test is performed in Malaysia for extra-pulmonary tuberculosis, providing the result after three days [3]. The radiometric methods have widespread practice e.g., TB screening by the United Kingdom (UK) Visas and Immigration (UKVI) office in Malaysia [4]. The UK National Health Service (NHS) uses chest X-ray to look for changes in the appearance of the lungs [5]. Urine and blood samples are checked for Extrapulmonary TB occurring outside of the lungs which may involve scanning the affected part of the body e.g. MRI, ultrasound scan or a biopsy. The tuberculin skin test (TST) can be also performed for latent TB [5].

Several studies employed machine learning techniques to assist in the diagnosis and monitoring of TB to offer a low-cost, simple, rapid and portable platform [6]. Various input data were analyzed such as tissue images [7], clinical symptoms and images from colorimetric-based tests [8], [9]. Analysis of the clinical symptoms requires the collection of many details over some period of time. Tissue images requires resources and expert knowledge. Osman, Mashor and Jaafar (2010) proposed a tuberculosis bacteria detection technique from tissue sample by Ziehl-Neelsen staining method. The prepared sample image from an optical microscope was segmented by moving k-mean clustering for tuberculosis bacteria extraction. Both RGB and C-Y colour were utilised to acquire a robust and improved segmentation under various staining condition. The hybrid multilayered perceptron network (HMLP) selected the features among the geometrical features of Zernike moments to detect tuberculosis bacteria. The result showed 98.0%, 100% and 96.19% of accuracy, sensitivity and specificity respectively to find the class of definite and possible TB.

However when it comes to low-cost, simple, rapid and portable detection of TB, lateral flow tests (LFTs) are more popular [10]. In theory, any coloured particle can be used for LFT, however latex (i.e. blue colour) or nanometer sized particles of gold (i.e. red colour) are most commonly used. Tsai, Shen, Cheng and Chen (2013) developed colorimetric sensing using unmodified gold nanoparticles and single-stranded detection oligonucleotides for a TB test. A smartphone was utilized to collect the multiple detection results of color variation from the concentration on cellulose paper and transmit the data to the cloud. Smart nanomaterials has been recently used in Plasmonic ELISA experiments [8]. Plasmonic ELISA enables the detection of a few molecules of analyte by the incorporation of smart nanomaterials for better sensitivity of the developed detection system.

In this research, we employ Plasmonic ELISA and computational intelligence to facilitate automatic diagnosis of TB. This study presents the initial phase of a project that aims to develop a mobile-based point-of-care (POC) platform for TB diagnosis. The plasmonic ELISA experiments were based on synthetic biological samples as well as real samples. Work is ongoing to apply plasmonic ELISA on more real samples (i.e., urine and saliva).

*This research is funded by the British Council Newton Institutional Links and Newton-Ungku Omar Fund.

K. J. AbuHassan, M. H. Tania and M. A. Hossain are with Anglia Ruskin IT Research Institute (ARITI), Anglia Ruskin University, Chelmsford Campus, CM1 1SQ, UK (Phone: +44(0)1245 68 3549; email: kamal.abu-hassan@anglia.ac.uk; marzia.hoque@pgr.anglia.ac.uk; alamgir.hossain@anglia.ac.uk).

N. M. Bakhori, N. Kusnin, U. Z. M. Azmi and N. A. Yusof are with the Institute of Advance Technology, University Putra Malaysia, 43400, UPM Serdang, Selangor, Malaysia (email: noremyliamb@gmail.com; norzilakusnin87@gmail.com; azahy@upm.edu.my)

N. A. Yusof is also with the Department of Chemistry, Faculty of Science, University Putra Malaysia, 43400, UPM Serdang, Selangor, Malaysia

B. A. Evans is with Norwich Medical School, University of East Anglia, Norwich, Norfolk, NR4 7TJ, UK (email: Benjamin.Evans@uea.ac.uk).

II. METHODS

A. Plasmonic ELISA

A batch of 96-well plates were coated with Mycobacterium tuberculosis ESAT-6-like protein EsxB (100 µL, Cusao) diluted 1:1000 in carbonate buffer (100 mM, pH 9.6) at 4°C overnight. After washing three times with wash buffer, the plates were blocked with blocking buffer for 2 hours at room temperature. Mouse monoclonal antibody (KFB42) to CFP10 (100 µL, Abcam), diluted 1:4000 in antibody diluent buffer, was added for 2 hours. The plates were then washed three times, and biotinylated goat polyclonal secondary antibody to mouse IgG2b was added (100 µL, Abcam), diluted 1:1000 in antibody diluent buffer, for 2 hours. After washing three times, 50 µL from stock solution of the streptavidin-catalase conjugate was diluted in 1.2 mL of antibody diluent buffer, then 100 µL was added into each well for 2 hours at room temperature [8]. The plates were then washed three times with wash buffer, twice with PBS and once with deionized water. Then, hydrogen peroxide (100 µL, 275 µM) in MES buffer (2-(N-morpholino)ethanesulphonic acid, 1 mM, pH 6.5) was added to each well of the plate. Immediately, freshly prepared gold (III) chloride trihydrate (100 µL, 0.2 mM) in MES buffer was added to each well. Photos were captured by using iPhone 5 camera (8-megapixel camera) at various distances between the mobile camera and the ELISA plates. These distances were non-predefined as the mobile device was not fixed by a holder. This has also caused blurriness in a number of images.

B. Color-based Image Classification

The image segmentation, feature extraction and image classification algorithms were coded in MATLAB. We have analysed images from 71 wells (35 are TB-positive and 36 are TB-negative). The performance of the classifiers were tested based on two approaches as described in section 3 below.

1) Image segmentation

The key steps in image segmentation are summarized in Algorithm 1 below.

Algorithm 1: Image Segmentation Using K-Means Clustering

Input: Images of plasmonic ELISA plates; number of clusters *k*

Output: segmented wells

Steps:

1) Read the images in Red-Green-Blue (RGB) color space
2) Convert the data into the CIELAB color space
3) Use colors in the AB space to measure the Euclidean distance for clustering
4) Repeat step 3 three time to avoid local minima
5) For clusters 1 to k, separate the objects using the index clustering. This will produce k images.
6) Identify the cluster that contains the colored wells.
7) Apply a noise filter. Pixels were thresholded based on L* and the number of connected pixels in each component.

Images were segmented using k-means clustering, thresholding and the CIE L*a*b* color space (CIELAB). CIELAB is an absolute three axis color model with one channel for lightness (L*) and two color channels (a* and b*). The lightness (L*) ranges from 0 (white) into 100 (black). Negative values of a* and b* corresponds to green and blue colors, respectively. Positive values of a* and b* corresponds to red and yellow colors, respectively. Each image was converted into CIELAB color space. Image segmentation was based on colors in the AB space only. K-means clustering was used to cluster the objects into six clusters based on the Euclidean distance metric.

2) Color-based feature extraction

Color histogram features were extracted from the segmented photos. Color histogram is a representation of the number of pixels at each intensity level of a color channel. The extracted histogram features were simple statistical features which reveal the global properties of the intensity level distribution for each color channel. The histogram can be represented as a probability distribution, *P(g)*, of the intensity levels (1) [12].

$$P(g) = N(g)/M \tag{1}$$

Where g is the intensity level, *N(g)* is the number of pixels at intensity level *g* and *M* is the total number of pixels. In our feature extraction algorithm, we calculated the mean, standard deviation, skewness, mode, and energy for each color channel (i.e. L*, a* and b*). The entropy for a* and b* color channels were also included in the feature pool, providing a total of 17 features for characterization of each well. Below we presented the equations for the mean, standard deviation, skewness, energy and entropy.

The mean ($\bar{g}$) reflects the overall intensity level in the image. The mathematical representation for the mean intensity level and the standard deviation (σ_g) is provided in (2) and (3), respectively.

$$\bar{g} = \sum_{g=0}^{W-1} gP(g) = \sum_r \sum_c I(r,c)/M \tag{2}$$

$$\sigma_g = \sqrt{\sum_{g=0}^{W-1} (g-\bar{g})^2 P(g)} \tag{3}$$

W is the number of intensity levels, r is the number of rows in the image and c is the number of columns in the image. The skew computes the asymmetry of the probability distribution of the histogram. Therefore, it reveals information about the shape of the distribution.

$$SKEW = \frac{1}{\sigma_g^3} \sum_{g=0}^{W-1} (g-\bar{g})^3 P(g) \tag{4}$$

The energy measure is related to the color span (i.e. the spread of the pixel values). The color energy (5) decreases as the pixel values span a wider intensity range. The entropy measure describes the required amount of information to code the image data. In contrast to the energy measure, the entropy increases as the pixel values span a wider intensity range. The mathematical representation for the entropy can be found in (6).

$$ENERGY = \sum_{g=0}^{W-1} [P(g)]^2 \quad (5)$$

$$ENTROPY = -\sum_{g=0}^{W-1} P(g) \log_2 [P(g)] \quad (6)$$

3) Image classification

We have used the Mathworks Classification Learner toolkit for image classification. The toolkit facilitates automatic training of the classification algorithms and validation of the outcome. We have tried various classifiers such as decision trees, support vector machines (SVMs), k-Nearest Neighbors algorithm (k-NN) classifiers and ensemble classifiers. The accuracy of the classifiers were tested based on two approaches. In the first approach, the dataset was divided randomly (by the Mathworks Classification Learner) into a training set (75%) and a testing set (25%). In the second approach, the full dataset were used to assess the accuracy of the classifiers based on five-fold cross-validation. This is an unbiased measure that divides all samples to 5 subsamples and then iteratively leaves one subsample out of training for subsequent testing until each of the 5 subsample are evaluated. We used five-fold cross-validation due to the small size of the dataset. The best classifier was finally tested with images from 6 wells containing real biological samples.

III. RESULTS

A. Plasmonic ELISA

Fig. 1 illustrates example images for a TB-negative (top) and a TB-positive (bottom) synthetic biological samples.

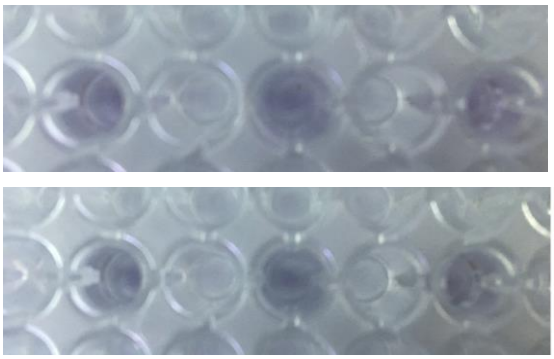

Figure 1. Sample photos of Plasmonic ELISA plates. The top photo was taken from a shorter distance. Top image is for a TB-negative sample. Bottom image is for a TB-positive samples.

B. Color-based Image Analysis

Fig. 2 illustrates a sample segmented image tagged with the steps of the segmentation algorithm. The accuracy of k-means clustering was 77.6%. This outcome is based on the accuracy of selecting the correct cluster. We have automatically chosen the cluster containing the wells based on the mean 'a*' and 'b*' value. In our experiments, we find that the cluster containing the blue and pink wells has the minimum mean value among all clusters (i.e., 6 clusters). Forty five images (i.e., 77.6%) out of fifty eight images were segmented automatically. The correct clusters for the other 13 images were then identified manually.

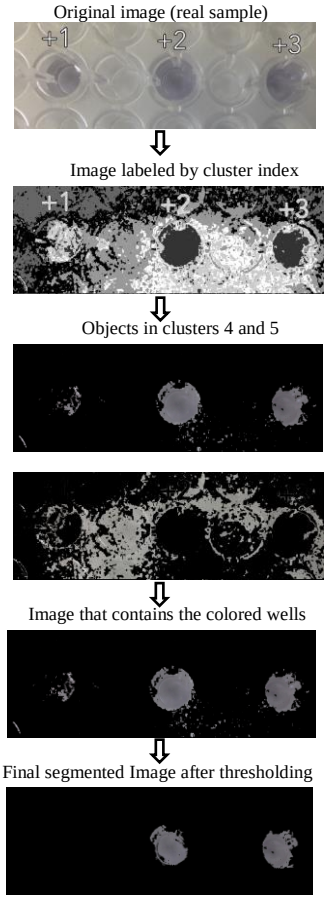

Figure 2. Sample result of segmentation. The plus sign (+) was used to label the image (positive TB). Only 2 clusters (out of 6) is presented.

As mentioned earlier, various classifiers (shown in Table. I) were trained by using 75% of the data. The performance of the classifiers were evaluated by using 25% of the data. The results in Table. I show that the ensemble (i.e., bagged ensemble trees) classifier achieved the best result (>94%). As mentioned earlier, the testing dataset was chosen randomly.

TABLE I. SUMMARY OF THE TESTING PERFORAMCE

Classifier	**Testing performance**		
	Accuracy (%)	***Sensitivity (%)***	***Specificity (%)***
Bagged trees	94.1	100	88.9
Boosted trees	82.4	100	66.7
Fine KNN	70.6	100	44.4
Cubic SVM	76.5	100	55.6
Medium decision tree	70.6	87.5	55.6

Training the classifiers with all data (i.e., 71 wells) showed a 97.2% accuracy rate achieved by the bagged ensemble trees. The five-fold cross-validation results are presented in Table. II. The best classifier was finally tested with images from 6 wells containing real physiological samples (3 were TB-positive and 3 were TB-negative). All images were correctly classified except one image for a TB-positive well which was misclassified as TB-negative.

TABLE II. SUMMARY OF FIVE-FOLD CROSS-VALIDATION RESULTS

Classifier	Testing performance		
	Accuracy (%)	*Sensitivity (%)*	*Specificity (%)*
Bagged trees	97.2	97.1	97.2
Boosted trees	93.0	97.1	88.9
Fine KNN	94.4	97.1	91.7
Cubic SVM	88.7	91.4	86.1
Medium decision tree	87.3	88.6	86.1

IV. DISCUSSION

In this paper we propose a novel study for automatic diagnosis of TB based on image classification and plasmonic ELISA. This research study has two research contributions. First, it integrates a biosensing mechanism (i.e. plasmonic ELISA) with computational intelligence to detect TB. Second, it compares the classification performance of various types of classifiers. The results of applying the classifiers on the testing dataset (25% of the whole dataset) show high accuracy rate (>94%) despite blurriness in the images. The bagged tree method uses random forest classifier with decision tree learners. We have varied the number of learners (100 – 300 learners) in our simulations but observed no significant change in the predictive performance.

Overall, the predictive accuracy was affected by the image acquisition approach. As mentioned earlier, photos were taken at various unknown distances between the mobile camera and the ELISA plates. In our experiments the mobile device was not fixed by a holder hence caused blurriness of some images. This challenge was tackled by converting the image into the CIELAB color space and then applying k-means clustering and thresholding algorithms. Hoffman et al. (2014) reported that expectation-maximization, k-means, and variational Bayesian inference all have the same performance, however, k-means take the minimum time to produce the result.

Plasmonic ELISA has potential for ultrasensitive detection promising wider, faster and low cost 24/7 real-time access for testing without experts. This technique usually uses a specific antibodies to capture target molecules (analyte) on a disposable substrate which is subsequently labelled with an enzyme, for instance through a biotin–streptavidin linkage. The biocatalytic cycle of the enzyme label is related to the growth of gold nanoparticles for the production of blue or pink colour due to the existence of the analyte. The blue colour appears in the presence of analyte. The enzyme catalase consumes hydrogen peroxide and slows down the kinetics of crystal growth. The pink colour appear when the gold ions are reduced by hydrogen peroxide at a fast rate.

Work is ongoing to apply plasmonic ELISA on more real samples (i.e., urine and saliva) in collaboration with Universiti Sains Malaysia Hospital. In the future work, the k-means segmentation algorithm will be optimized in terms of accuracy and speed, and compared with other segmentation methods such as graph cut segmentation [14]. The classifiers will be trained and tested with larger datasets. Mobile holders will be used for capturing imaging and video data. The parameters of the classifiers will be tuned and investigated in order to find the optimal model. Our overall aim is to develop a smartphone-based expert system for testing TB in real-time.

ACKNOWLEDGMENT

This is a collaborative research project between Anglia Ruskin University (UK) and University Putra Malaysia (Malaysia). The authors would like to thank Dr Mohammad Abdullah Al-Mamun from Cornell University for contributing to discussions about this work.

REFERENCES

[1] M. Raviglione and G. Sulis, "Tuberculosis 2015: Burden, Challenges and Strategy for Control and Elimination.," *Infect. Dis. Rep.*, vol. 8, no. 2, p. 6570, Jun. 2016.

[2] WHO, "Global tuberculosis report 2016," World Health Organization, 2017.

[3] Malaysian Thoracic Society, "Guidelines on Management of Tuberculosis," 2012. [Online]. Available: http://www.mts.org.my/Guidelines_TB.html#DIAGNOSIS. [Accessed: 02-Feb-2017].

[4] GOV.UK, "Tuberculosis testing in Malaysia," 2014. [Online]. Available: https://www.gov.uk/government/publications/tuberculosis-test-for-a-uk-visa-clinics-in-malaysia/tuberculosis-testing-in-malaysia. [Accessed: 03-Feb-2017].

[5] NHS, "Tuberculosis (TB) - Diagnosis - NHS Choices." [Online]. Available: http://www.nhs.uk/Conditions/Tuberculosis/Pages/Diagnosis.aspx. [Accessed: 12-Jan-2017].

[6] B. H. Tracey, G. Comina, S. Larson, M. Bravard, J. W. López, and R. H. Gilman, "Cough detection algorithm for monitoring patient recovery from pulmonary tuberculosis.," *Conf. Proc. ... Annu. Int. Conf. IEEE Eng. Med. Biol. Soc. IEEE Eng. Med. Biol. Soc. Annu. Conf.*, vol. 2011, pp. 6017–20, Jan. 2011.

[7] M. K. Osman, M. Y. Mashor, and H. Jaafar, "Detection of mycobacterium tuberculosis in Ziehl-Neelsen stained tissue images using Zernike moments and hybrid multilayered perceptron network," in *2010 IEEE International Conference on Systems, Man and Cybernetics*, 2010, pp. 4049–4055.

[8] R. de la Rica and M. M. Stevens, "Plasmonic ELISA for the ultrasensitive detection of disease biomarkers with the naked eye.," *Nat. Nanotechnol.*, vol. 7, no. 12, pp. 821–4, Dec. 2012.

[9] E. F. O'Connor, S. Paterson, and R. de la Rica, "Naked-eye detection as a universal approach to lower the limit of detection of enzyme-linked immunoassays," *Anal. Bioanal. Chem.*, vol. 408, no. 13, pp. 3389–3393, 2016.

[10] J. S. Sutherland, J. Mendy, A. Gindeh, G. Walzl, T. Togun, O. Owolabi, S. Donkor, M. O. Ota, E. T. Kon Fat, T. H. M. Ottenhoff, A. Geluk, and P. L. A. M. Corstjens, "Use of lateral flow assays to determine IP-10 and CCL4 levels in pleural effusions and whole blood for TB diagnosis," *Tuberculosis*, vol. 96, pp. 31–36, 2016.

[11] T.-T. Tsai, S.-W. Shen, C.-M. Cheng, and C.-F. Chen, "Paper-based tuberculosis diagnostic devices with colorimetric gold nanoparticles," *Sci. Technol. Adv. Mater.*, vol. 14, no. 4, p. 44404, 2013.

[12] S. Sergyan, "Color histogram features based image classification in content-based image retrieval systems," in *2008 6th International Symposium on Applied Machine Intelligence and Informatics*, 2008, pp. 221–224.

[13] R. A. Hoffman, S. Kothari, and M. D. Wang, "Comparison of normalization algorithms for cross-batch color segmentation of histopathological images," *Conf. Proc. ... Annu. Int. Conf. IEEE Eng. Med. Biol. Soc. IEEE Eng. Med. Biol. Soc. Annu. Conf.*, vol. 2014, pp. 194–197, 2014.

[14] M. B. Salah, A. Mitiche, and I. B. Ayed, "Multiregion Image Segmentation by Parametric Kernel Graph Cuts," *IEEE Trans. Image Process.*, vol. 20, no. 2, pp. 545–557, Feb. 2011.